Princeton Plasma Physics Laboratory

PPPL- 4540

PPPL- 4540

New Classes of Quasi-helically Symmetric Stellarators

L.P. Ku and A.H. Boozer

August, 2010

Prepared for the U.S. Department of Energy under Contract DE-AC02-09CH11466.

Princeton Plasma Physics Laboratory
Report Disclaimers

Full Legal Disclaimer

Trademark Disclaimer

PPPL Report Availability

Princeton Plasma Physics Laboratory:

http://www.pppl.gov/techreports.cfm

Office of Scientific and Technical Information (OSTI):

http://www.osti.gov/bridge

Related Links:

U.S. Department of Energy

Office of Scientific and Technical Information

Fusion Links

New classes of quasi-helically symmetric stellarators

L. P. Ku[1] and A. H. Boozer[2]
[1]Princeton Plasma Physics Laboratory, Princeton University, Princeton, NJ 08543
[2]Columbia University, New York, NY 10027

E-mail: lpku@pppl.gov

Abstract
New classes of quasi-helically symmetric stellarators with aspect ratios ≤ 10 have been found which are stable to the perturbation of magnetohydrodynamic modes at plasma pressures of practical interest. These configurations have large rotational transform and good quality of flux surfaces. Characteristics of some selected examples are discussed in detail. The feasibility of using modular coils for these stellarators has been investigated. It is shown that practical designs for modular coils can be achieved.

PACS: 52.55Hc, 52.55.-s, 28.52.-s

1. Introduction

The existence of quasi-helically symmetric stellarators (QHS) was first discovered by Nuhrenberg and Zille [1]. In these configurations the three dimensional magnetic field strength $B(s,\theta,\phi)$ takes on the two dimensional form $B(s,\theta-\phi)$ that gives a conserved canonical momentum [2]. The discovery gives the hope that stellarator reactors with excellent confinement of particles at high plasma pressures could be realized. An experimental device HSX [3] is investigating quasi-helical symmetry at a low plasma beta, $\beta=2\mu\langle p/B^2\rangle$.

Although particle orbits are strictly confined in a purely quasi-helically symmetric configuration in the sense that the orbits deviate from flux surfaces by no more than a banana width, configurations that can be practically devised at finite pressures and at reasonable plasma aspect ratios often only approximately satisfy the quasi-helical condition. The approximation breaks helical symmetry, hence degrades particle confinement. The symmetry breaking due to the finite aspect ratio scales as the aspect ratio inverse to the third power [4]. The nominal aspect ratio for HSX is 8. The optimization for magnetohydrodynamic (MHD) stability may also introduce non-helical components in the magnetic spectrum that perturb the quasi-symmetry, further degrading the particle confinement.

The purpose of this paper is to document our recent discoveries of classes of QHS that have relatively small aspect ratios (<10) and good MHD stability characteristics at reasonably high beta that still retain good quasi-symmetry. These qualities render these configurations competitive as candidates for future experimental devices and fusion power reactors.

In the following, section II discusses in detail the physics properties of a four field-period configuration with an aspect ratio 8. Section III introduces a five field-period, aspect ratio 10 configuration optimized for 10% β that has equally attractive properties. Section IV discusses configurations having aspect ratio 6 in three field periods, which appears to be close to the smallest aspect ratio for acceptable QHS configurations. Section V presents a cursory study of coils for the configurations. Example modular coils are shown for the four field period configuration. Section VI provides conclusions and a summary.

2. QHS with N_p=4 and A_p=8

2.1. Configuration characteristics

We begin with a class of QHS that has an aspect ratio A_p= 8 in four field periods (N_p=4). Here, $A_p=R_p/a_p$, where R_p and a_p are the average plasma major and minor radius, respectively. A representative configuration is shown in figure 1 whose boundary shape may be described mostly by the eight terms in the Garabedian representation [5]

$$R + iZ = e^{2\pi iu} \sum \Delta_{m,n} e^{-2\pi i(mu-nv)} \tag{1}$$

as follows: $\Delta_{2,1}$=-0.596, $\Delta_{1,1}$=0.595, $\Delta_{-1,-1}$=0.287, $\Delta_{1,-1}$=0.105, $\Delta_{3,1}$=0.089, $\Delta_{2,2}$=-0.073, $\Delta_{1,2}$=0.073 and $\Delta_{0,1}$=0.050. In this representation the term defining the minor radius, $\Delta_{0,0}$, is normalized to 1.0. In equation (1), *R* and *Z* are the radial and axial components of cylindrical coordinates, *m* and *n* are the poloidal and toroidal mode numbers, and *u* and *v* are the normalized poloidal and toroidal angle-like variables, $0 \le u \le 1$, $0 \le v \le 1$ ($2\pi u=\theta$, $2\pi v/N_p=\phi$, θ and ϕ being the poloidal and toroidal angles, respectively). The nearly identical values of $\Delta_{2,1}$ and $\Delta_{1,1}$ lead to elongated shapes in almost all cross sections, giving a distinctive signature to this class of configurations. The top and perspective views of the configuration are shown in figure 2 with the variation of the magnetic field strength illustrated. The large $\Delta_{1,1}$ generates a large torsion for the magnetic axis so that the rotational transform is large, ~1.25, or 0.32 per field period, in the absence of the plasma pressure. The rotational transform is nearly uniform throughout the plasma volume. The radial dependence of the rotational transform is given in figure 3, in which we also show a possible variation of the rotational transform when the pressure and bootstrap currents are included at 4% β. The details of the rotational transform at a finite pressure depend on the temperature and density profiles. The pressure profile used in figure 3 is taken from NCSX [6] in the form

$$p(s) = (1 - s^{2.23})^{1.84} \tag{2}$$

where *s* is the normalized toroidal flux. The bootstrap current was calculated using the BOOTSJ code [7] which is applicable in the low collisionality regime. We have assumed a flat density profile with n_0R_p/T_0^2~0.05 (or equivalently ν^*~0.01) where n_0 and T_0 are the central density and temperature and R_p is the plasma major radius. The magnitude of the current is ~0.012 MA-Wb/m, giving an internally generated rotational transform ~0.07. The direction of the current is such that the internally generated rotational transform opposes the externally supplied one. The radial profile of the rotational transform decreases from ~1.3 at the magnetic axis to ~1.1 near the edge at 4% β. A second order resonance 2/7 appears at about 80% of the radius whose effect on the quality of flux surfaces is shown in figure 4 based on PIES [8] calculations. The island width due to this resonance is very small and the loss of flux is essentially negligible within the framework of fixed-boundary calculations.

The quasi-helical nature of the configuration may be understood by examining the residues in the magnetic spectrum defined as the non-helical components in the Fourier spectrum in a coordinate system in which the Jacobian is proportional to $1/B^2$, the so-called Boozer coordinates [9]. It may also be checked by examining the contours of field strength B on flux surfaces. Examples are given in figure 5 for the residues as a function of the plasma radius. In this figure the dominant helical component $B_{1,1}$ is also included for comparison. Here, we represent the magnetic field harmonics as $B_{m,n}$, where the first subscript is the poloidal mode number and the second the toroidal mode number. The "noise" content in the magnetic energy due to the residues is about 0.2% at the half-radius of the plasma and is about 2.5% at the edge of the plasma. These noise levels in terms of the magnetic energy are defined as the square root of the sum of the squares of the magnetic field strength of the residues divided by the square root of the sum of the squares of the field strength of the helical terms. The significant residue components are $B_{0,1}$, $B_{2,0}$, and $B_{2,1}$ with their magnitudes being ~1.8%, 1.3% and 0.9%, respectively, when compared to the field strength on the magnetic axis. An example of the |B| contour on the flux surface at about 70% of the plasma radius is shown in figure 6. We see that, qualitatively, the field strengths deviate only slightly from the quasi-helical symmetry.

2.2. Transport and confinement properties

Given the good quasi-helical quality of the configuration, we expect that the configuration should have excellent particle transport and confinement properties, consistent with the theory. In figure 7 we show the variation of |B| as we follow a magnetic field line on a surface at about 70% of the radius. We note that the field strength has nearly a constant maximum and minimum along the segment that we followed and the symmetry condition $B(l)=B(L+l)$ is well satisfied. Here, l is the distance along a field line and L is a constant. The diffusion coefficient for the neo-classical transport estimated by using DKES [10] is shown in figure 8 for the 70%-radius surface for mean-free-paths ranging from 10^5 to 10 m for 1 keV ions. The radial electric field has been taken to be zero in the calculation. The diffusion coefficient at this radius is ~0.02 m^2/s for the collisionality ν/v_{th}~0.001 in a device having an average minor radius a_p~1 m and magnetic field strength ~1.2 T. It is about an order of magnitude larger if the collisionality is increased by two orders of magnitude. The effective helical ripples calculated by NEO [11] are shown in figure 9. They are considerably less than 1% in the bulk of the plasma volume. Confinement of fast ions is excellent. An example calculation using ORBIT [12] for the α particle loss in a hypothetic reactor with 1000 m^3 volume, 5 T field, 4% beta and a central collisionality n_0R_p/T_0^2= 0.2, gives an energy loss fraction of about 2.5%. For a given set of density and temperature profiles the fusion power scales as $B^4\beta^2R_p^3/A_p^2$. Using the same form factors as those used in ARIES-CS [13] which is a power plant for the low aspect ratio, quasi-axisymmetric stellarators, the conditions used for the hypothetical reactor give a thermal power of about 1200 MW in a steady state.

2.3. MHD stability properties

The configuration is optimized to have favorable MHD stability characteristics to the external kink, ballooning and Mercier modes at 4% beta. This is achieved by modifying the boundary geometric coefficients such that stability is attained as indicated by the linear stability code calculations. The external kink modes, infinite-n ballooning and Mercier modes were analyzed using Terpsichore [14], COBRA [15] and VMEC [18], respectively. The underlying equilibrium was calculated by VMEC with 7 poloidal modes, 6 toroidal modes and 49 flux surfaces. Two field lines were used in the integration of the ballooning equation: that passing through the toroidal angle at the beginning of a period and that at the half period at poloidal angles corresponding to the outboard midplane. In the global kink stability calculation, families of N=0, 1 and 2 modes were analyzed and for N=1 both even and odd parities were studied. However, the number of perturbation modes used was limited (~90). Because the Mercier solution is strongly

affected by local resonances, isolated instabilities on single surfaces, if present, were general ignored.

If the plasma beta is increased to 5-6% while keeping the boundary shape fixed, we find that the kink stability is not strongly affected, but the Mercier and infinite-n ballooning modes become unstable. This is partly due to the configuration lacking a deep magnetic well. At 5% beta Mercier is generally stable in the outer half of the radius and the unstable region for the ballooning modes occupies ~15% of the plasma radius. Since many stellarator experiments have succeeded in operating above the linear stability threshold and the recent theoretical work by Cooper has shown that the ballooning instability threshold would be higher when kinetic effects are included in the formulation [17], it is hopeful that the actual stability threshold of this configuration would in fact be higher than the 4% beta where the configuration was optimized.

3. QHS with N_p=5 and A_p=10

The configuration discussed in the previous section is now shown to belong to a family whose members are also found at higher aspect ratios and beta. We wish to document, in particular, a configuration of five field periods having an aspect ratio 10. This configuration, whose cross sections of the last closed magnetic surface are shown in figure 10, has been optimized to be MHD stable at 10% β with respect to the external kink modes, ballooning modes and Mercier modes. A top view and perspective view of the configuration are shown in figure 11. The boundary shape may be described mostly by $\Delta_{1,1}$=0.588, $\Delta_{2,1}$=-0.545, $\Delta_{-1,-1}$=0.304, $\Delta_{3,1}$=0.080, $\Delta_{-1,1}$=-0.050, $\Delta_{-1,0}$=0.049, $\Delta_{2,-1}$=0.048, $\Delta_{1,2}$=0.046, $\Delta_{3,2}$ =0.044, and $\Delta_{1,-1}$=0.043 in the Garabedian representation. The rotational transform is in the range of 1.33 to 1.54 from the magnetic axis to the plasma edge at zero pressure. At 10% β, the transform profile is modified by the bootstrap and Pfirsch-Schluter currents to be in the range of 1.38 to 1.19 using the pressure and current profiles discussed in section 2. A second order resonance 2/7 exists at ~80% of the radius without the plasma pressure and a first order 1/4 resonance appears approximately at 50% of the plasma radius when the pressure and currents are present. The island widths and the overall flux surface quality have been analyzed by using the PIES code. A plot showing the flux surfaces at the crescent shaped section is illustrated in figure 12. Without the plasma pressure, the natural 2/7 island chain occupies about 5% of the radius. At 10% β the 1/4 resonance does not appear to open up islands of any significant degree within the framework of the fixed boundary PIES analysis. The total width occupied by various island chains is about 6%, including the 1/4, 2/7 and 3/13 resonances. The rotational transform calculated by PIES at 10% β deviates only slightly from that calculated by VMEC, 1.42 versus 1.39 near the axis and 1.20 versus 1.19 at the plasma boundary. In the optimization process we did not particularly attempt to minimize the parallel component of the plasma current. The rotational transform is sufficiently high that even at 10% β the axis shift at this aspect ratio amounts to only ~3% of the minor radius overall and ~10% of the half-width at the crescent-shaped section. With carefully designed coils, it is expected that good flux surfaces could be maintained at this beta value.

The configuration contains a fairly large mirror field, $B_{0,1}$, the largest one, which occurs at the plasma boundary, is ~4.0% when normalized to the field strength at the magnetic axis. It also has noticeable $B_{2,1}$ and $B_{2,0}$ terms in the magnetic spectrum, ~2.0% and 1.2% at the plasma boundary, respectively. Nevertheless, these perturbations do not seriously threaten the overall confinement. The effective helical ripple is about 0.5% at the 70% radius and is less than 1.5% overall. An ORBIT calculation for the loss of alpha particles in a hypothetic reactor of 1000 m^3 volume gives an energy loss fraction of ~2% with the same conditions discussed in section 2. Because of the higher beta in this case, the hypothetic reactor would yield a thermal output almost six times as much as the 4% β, N_p=4 case in section 2. For smaller power outputs at the same β,

either the volume or the magnetic field may be reduced. Both will result in larger losses of alpha particles. The best combination of the plasma beta, major radius and the magnetic field for a reactor will ultimately be determined by systems tradeoffs.

The family of configurations discussed above is not the only one we've found that have good quasi-symmetry and MHD stability properties. In figure 13 we show another possible configuration that may also be of interest. This family of configurations is characterized by $\Delta_{2,1}$= -0.545, $\Delta_{1,1}$=0.510, $\Delta_{-1,1}$=0.291, $\Delta_{-2,0}$=-0.117, $\Delta_{-1,0}$=0.085, $\Delta_{0,1}$=0.051, $\Delta_{4,1}$=0.051, $\Delta_{2,2}$=0.050, and $\Delta_{1,2}$=-0.040. This configuration is designed to be stable to the kink, ballooning and Mercier modes at 4% β. The residues are small, the largest two being $B_{0,1}$ and $B_{2,1}$, 1.3% and 0.8% respectively. The noise content due to the residues is about 2% at the last flux surface and the effective ripple at the 70% radius is only 0.35%.

4. QHS with N_p=3, A_p=6

While quasi-helical symmetry can be better attained at larger aspect ratios, it is not clear where the lower practical limit is. We have studied configurations with aspect ratio as low as 6 in three field periods and found that with somewhat relaxed requirements for the MHD stability reasonably good quasi-symmetry can still be achieved. When the requirements for MHD stability at high β are included in the configuration optimization, the quality of quasi-symmetry is significantly compromised to the point where attractive practical devices may not be easily found. In the following, we shall illustrate a configuration that has a calculated beta limit of ~2% but with acceptable quasi-symmetry.

In figure 14 we show the cross sections of the last closed flux surface for a configuration described by $\Delta_{1,1}$=0.712, $\Delta_{2,1}$=-0.653, $\Delta_{1,-1}$=0.305, $\Delta_{-1,-1}$=0.269, $\Delta_{0,1}$=0.139, $\Delta_{2,2}$=-0.129, $\Delta_{1,2}$=0.117, $\Delta_{2,0}$=-0.086, $\Delta_{3,1}$=0.049, $\Delta_{-1,0}$=0.036. There are many terms with magnitude greater than 10% of $\Delta_{0,0}$, resulting in a stronger shaping in this configuration than both the four field period, A_p=8 configuration and the five field period, A_p=10 configuration discussed in the previous sections although they do have a certain resemblance. A top view and perspective view of the configuration are given in figure 15. The rotational transform is ~0.95 and has a tokamak-like shear. The configuration has a deep magnetic well in the absence of plasma pressures, ~6%, so that the Mercier mode is very stable at β ~4%. The configuration, however, is not stable to the ballooning modes based on the analysis of the infinite-n COBRA code at this pressure; the stable condition is met at about β~2%. The effective ripple is small, ~0.2% at 70% radius, and the residues in the magnetic spectrum are also small, the largest ones being the mirror term $B_{0,1}$ which amounts to ~2% at the plasma boundary and $B_{2,1}$ which is about 1.2%. The overall content of the noise magnetic energy due to the non-helical components is quite low, ~2.5% at the boundary. The energy loss fraction of the fusion alphas in a hypothetic reactor is higher, however; about 10%, compared to ~2% loss in the A_p=8 and A_p=10 configurations at similar conditions, but the loss probably is still acceptable and can be reduced by increasing the magnetic field strength or making the plasma more collisional. Calculations of neo-classical diffusion coefficients using DKES showed that the coefficients are similar to the A_p=8 configuration in high collisionality regimes but in the long mean-free-path regions the diffusion coefficients of this case tend to be larger, e.g. ~2 when $\nu/v_{th} = 10^{-4}$ without imposing a radial electric field.

The search for configurations that satisfy the MHD stability conditions at 4% beta, especially those stable to the infinite-n ballooning modes on all flux surfaces, turned out to be rather difficult. A certain compromise of the quasi-symmetry needs to be made. An example is given in figure 16 which is calculated to be MHD stable at 4% beta but it has a large $B_{0,1}$ (~5.5%) and $B_{2,1}$ (~3.2%) in the magnetic spectrum with the overall noise energy content increased to

about 7% near the plasma edge. A clear indication of the degradation in the quasi-helical symmetry is the damage to the particle confinement. For example, the diffusion coefficients calculated by DKES are an order of magnitude larger in the low collisionality regimes than for the A_p=6 case discussed above. In the high collisionality regimes, the differences in neo-classical diffusion become smaller, about 2 between these two cases. Stellarators may be operated at higher densities and lower temperatures in fusion reactors than tokamaks. Additional optimization may yield configurations of aspect ratio 6 of interest for the design of a smaller power plant, but it appears that an aspect ratio ~6 may be the practical lower limit for quasi-helically symmetric devices.

5. Coils

Preliminary coil designs have been attempted using the NESCOIL [18] approach in which coils are placed on a winding surface approximately conformal to the last closed magnetic surface but it is separated from the plasma boundary by a chosen distance. The strong helical nature of the QHS configuration implies pairs of helical windings would be a good candidate for the primary coil system. But here, instead, we look into modular coils as the primary system as they are considered to be more practical in a power reactor. We shall illustrate the general features for the N_p=4, A_p=8 configuration discussed in section 2.

In figure 17 are top views of two sets of modular coils. The two sets of coils differ in the distance separating the winding surface from the boundary of the plasma. Both have four sets of coils in one field period with equal current in them. The two different separation distances correspond to the smallest radial build (~1.3 m) required for radiation shielding to protect coils from permanent damage and the nominal build (~1.8 m) required for having both tritium breeding blanket and radiation shielding in a 1000 m^3 reactor. Because of the rapid decay of high order harmonics in the magnetic fields produced by the current in coils, the geometry of the coils corresponding to the larger separation is much more complex. The picture is easier to see if we look at the coil contours in a plane defined by the poloidal and toroidal angles on the winding surface. This is given in figure 18. Some of the complexity arises from magnetic field distributions that are not important in determining the desired physics properties. These distributions may be filtered out using the singular value decomposition technique, as discussed in [19].

The last closed flux surface constructed using VMEC with the magnetic fields from the first set of coils is given in figure 19. Magnetic field ripples due to the discrete coils were removed in the calculation by using many filaments instead of the four coil sets with some assumed dimensions. The reconstructed plasma reproduced most of the quality of the original configuration, but it was not perfect. The algorithm for the solution of the current potential uses an equally spaced grid structure for the poloidal and toroidal angles. Such a structure leads to densely populated points near the tip of the cross section at the half-period for this configuration. The process of minimizing the normal field on the plasma surface gives rise to a large residue magnetic field error there. Also, the number of modes used in solving the current potential on the winding surface from which the coils were derived was limited (7 poloidal and 5 toroidal modes). This further introduced errors for the magnetic fields needed to support the plasma with the designed physics properties. Similar observations apply to the re-construction using the second sets of coils as well as the coils designed for configurations of other aspect ratios. Clearly, further optimization of the coils needs to be made, perhaps, using the similar procedures that were employed for designing NCSX or ARIES-CS.

6. Summary and conclusions

New quasi-helically symmetric configurations with aspect ratios less than 10 have been found that are stable to the MHD modes in both the short and long wave-length regimes at plasma beta values of practical interest. These configurations have large rotational transform due to the large torsion from the magnetic axis movement. They also have good quality of flux surfaces despite the existence of some low order resonance when the bootstrap currents are taken into account. As the aspect ratio is reduced to ~6 finding configurations of good quality becomes increasingly difficult. Much of the configuration landscape still remains to be explored, but it seems that the constraint of the aspect ratio placed on the attainability of quasi-helical symmetry will prevent us finding configurations at much lower values of A_p, especially when the MHD stability constraints are also imposed.

The feasibility of using modular coils for QHS has been investigated and the constructability of free-boundary equilibrium using these coils has been studied with respect to preserving the optimized physics properties of the fixed-boundary target equilibrium. Coil optimization has not been done and is necessary, but the initial study indicates designing practical modular coils is feasible. Other coil types may be more appropriate, particularly, a combination of helical coils, saddle coils and planar TF coils. Such studies will be the next step in our investigation.

Quasi-helically symmetric stellarators have not been considered as candidates for power producing reactors in recent years. The closest to QHS that have been pursued are those optimized to eliminate all forms of parallel currents, the iso-dynamic W7X and the HSR reactors with linked mirrors. The lower aspect ratio QHS we have found, with their attractive MHD stability and particle confinement properties, should make them competitive candidates in the consideration of future stellarator devices or power plants.

Acknowledgements

This work was supported by U. S. Department of Energy through the grant ER54333 to Columbia University and the contract DE-AC02-09CH11466 to the Princeton Plasma Physics Laboratory.

References

1. Nuhrenberg J and Zille R 1988 *Physics Letters A* **129(2)** 113
2. Boozer A H 1983 *Phys. Fluid* **26** 496
3. Canik J M, Anderson D T, Anderson F S B, Clark C, K. Likin M, Talmadge J N and Zhai K 2007 *Phys. Plasmas* **14**, 056107
4. Garren D A and Boozer A H 1991 *Phys. Fluid* **B3** 2822
5. Bauer F, Betancourt O and Garabedian P 1984 *"Magnetohydrodynamic Equilibrium and Stability of Stellarator,"* Springer-Verlag, New York
6. M. C. Zarnstorff, L. A. Berry, A. Brooks, E. Fredrickson, G. Y. Fu, S. Hirshman, S. Hudson, L. P. Ku, E. Lazarus, D. Mikkelsen, D. Monticello, G. H. Neilson, N. Pomphrey, a. Reiman, D. Spong, D. Strickler, A. Boozer, W. A. Cooper, R. Goldston, R. Hatcher, M. Isaev, C. Kessel, J. Lewandowski, J. F. Lyon, P. Merkel, H. Mynick, B. E. Nelson, C. Nuehrenberg, M. Redi, W. Reiersen, P. Rutherford, R. Sanchez, J. Schmidt and R. B. White, Plasma Phys. Control. Fusion 43, A237 (2001).
7. Shaing K C, Carreras B A, Dominguez N, Lynch V E, Tolliver J S 1989 *Phys. Fluids* **B1** 1663
8. Reiman A and Greenside H 1986 *Comput. Phys. Commun.* **43** 157
9. Boozer A H 1981 *Phys. Fluids* **24** 1999
10. Rij W I van and Hirshman S P 1989 *Phys. Fluids* **B1**, 563
11. Nemov V V, Kasilov S V, Kernbichler W and Heyn M F 1999 *Phys. Plasma* **6** 4622
12. White R B and Chance M S 1984 *Phys. Fluids* **27** 2455
13. Najmabadi F, Raffray A R and ARIES-CS Team 2008 *Fusion Science and Technology* **54(3)** 655
14. Anderson D T, Cooper W A, Gruber R, Merazzi S and Schwenn U 1990 *Scient. Comput. Supercomput.* **II**, 159
15. Sanchez R, Hirshman S P, Whitson J C and Ware A S 2000 *J. Comput. Phys,* **161** 589
16. Hirshman S P, Rij W I van and Merkel P 1986 *Comput. Phys. Commun.* **43** 143
17. Brocher L, Cooper W A, Graves J P, Cooper G A, Narushima Y, Watanabe K Y 2010 *Nuclear Fusion* **50** 025009
18. Merkel P 1987 *Nuclear Fusion* **27(5)** 867
19. Ku L P and Boozer A H 2010 "*Application of a boundary perturbation method to the study of field error effects in quasi-symmetric stellarators*" To be published

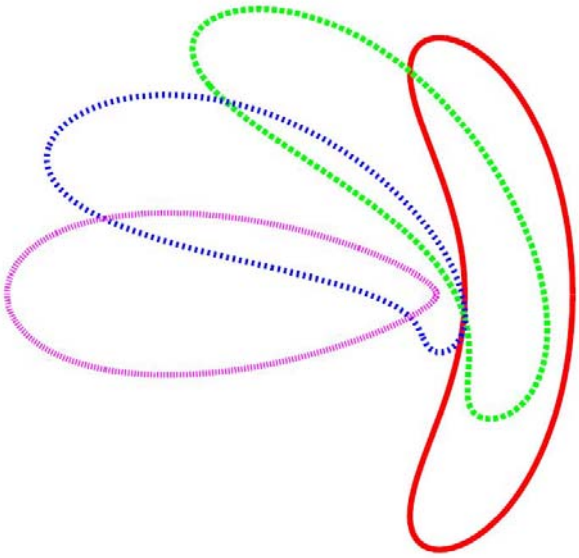

Figure 1. Cross sections of the last closed magnetic surface in four equally spaced toroidal angles for the N_p=4 and A_p=8 QHS.

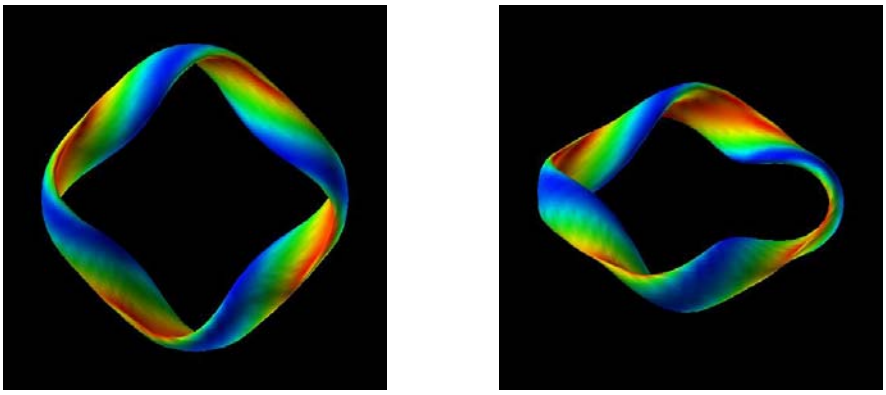

Figure 2. Top and perspective views of the N_p=4, A_p=8 QHS with the magnetic field strength shown in colored contours.

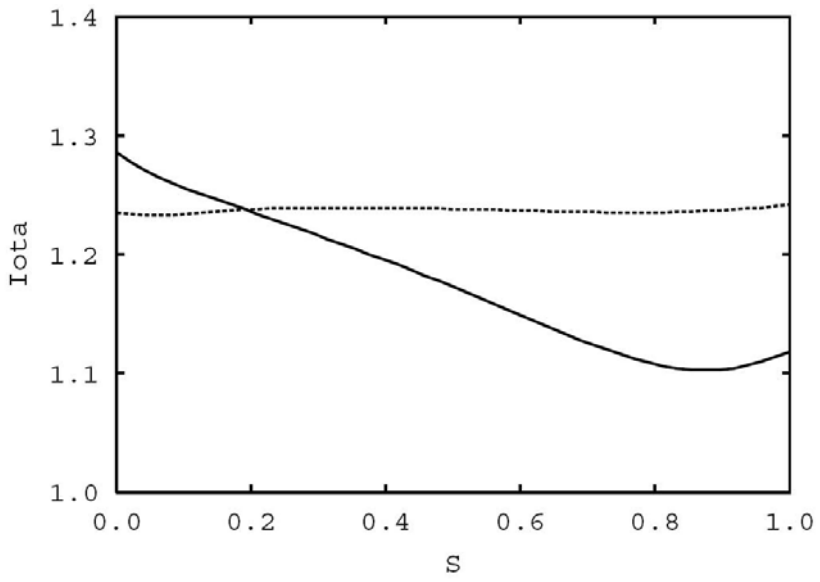

Figure 3. Rotational transform for the N_p=4, A_p=8 QHS as a function of the normalized toroidal flux ($\sim r^2/a_p^2$). The dotted curve is the transform due to the shaping without the plasma and the solid curve includes the effects of pressure and currents at $\beta \sim 4\%$.

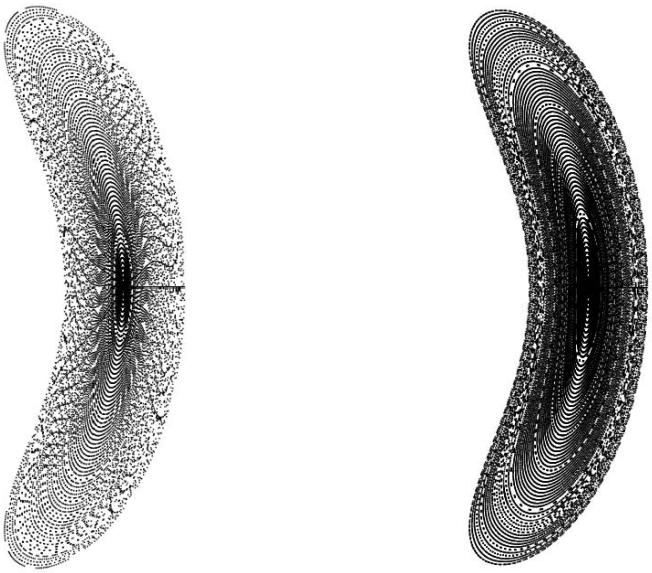

Figure 4. Poincaré plots showing the quality of flux surfaces for the N_p=4, A_p=8 QHS. The left frame is without plasma pressure and currents and the right frame includes the finite pressure effects at 4% β.

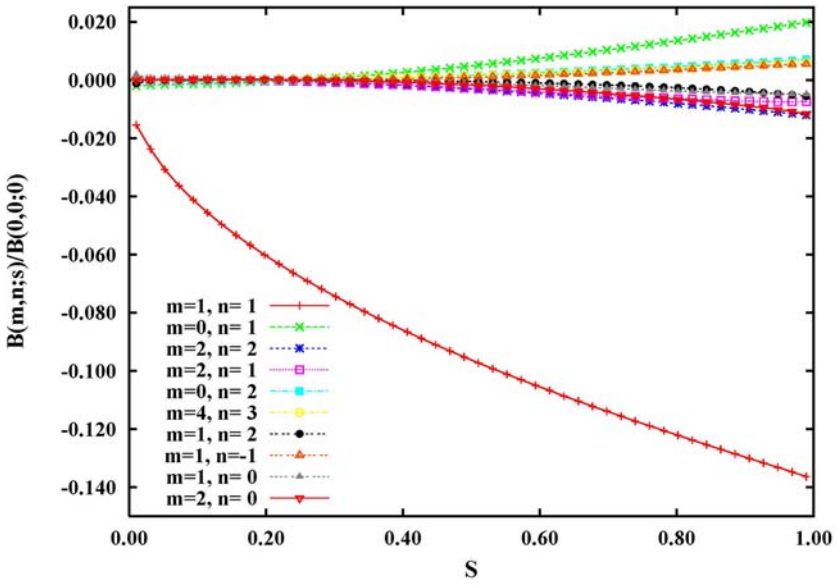

Figure 5. The significant magnetic field harmonics plotted as function of the normalized toroidal flux for the N_p=4, A_p=8 QHS.

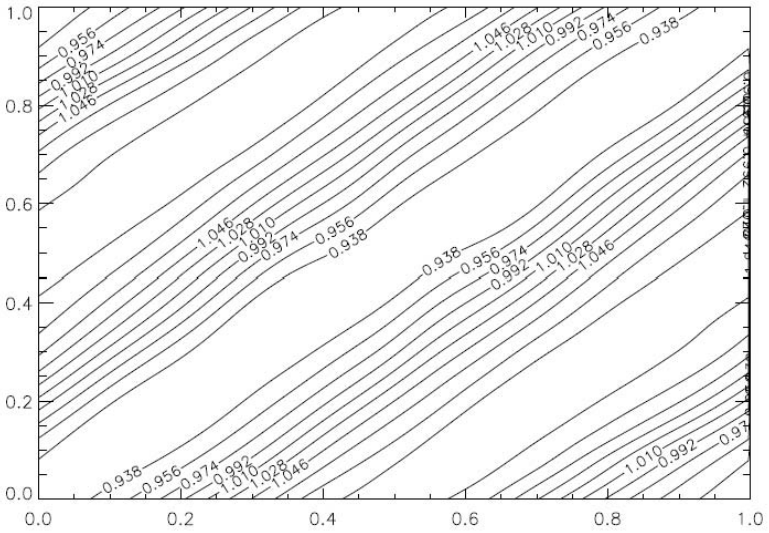

Figure 6. Magnetic field strength on a flux surface at ~70% of the radius for the N_p=4, A_p=8 QHS displayed in the coordinates defined by the toroidal angles, the abscissa, and poloidal angles, the ordinate.

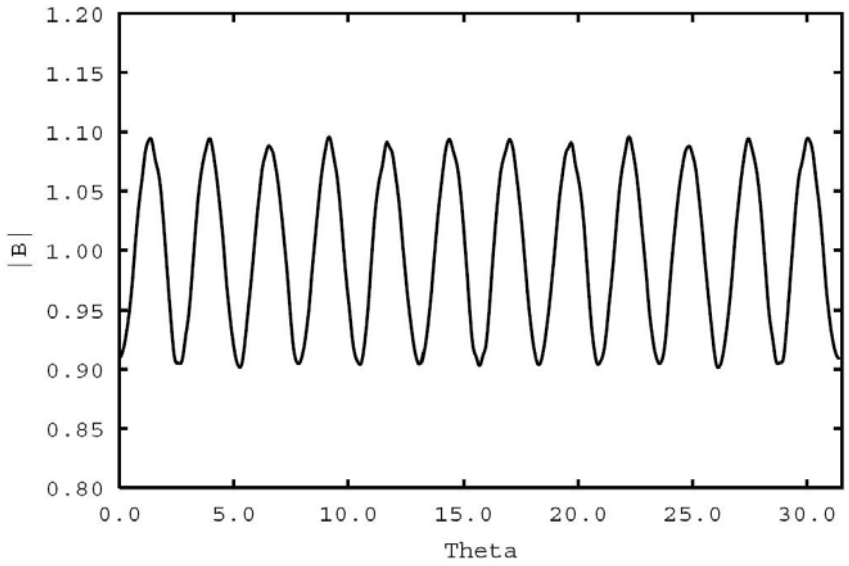

Figure 7. The magnetic field strength along a segment of field line for five poloidal circuits for the N_p=4, A_p=8 QHS at ~70% of the radius.

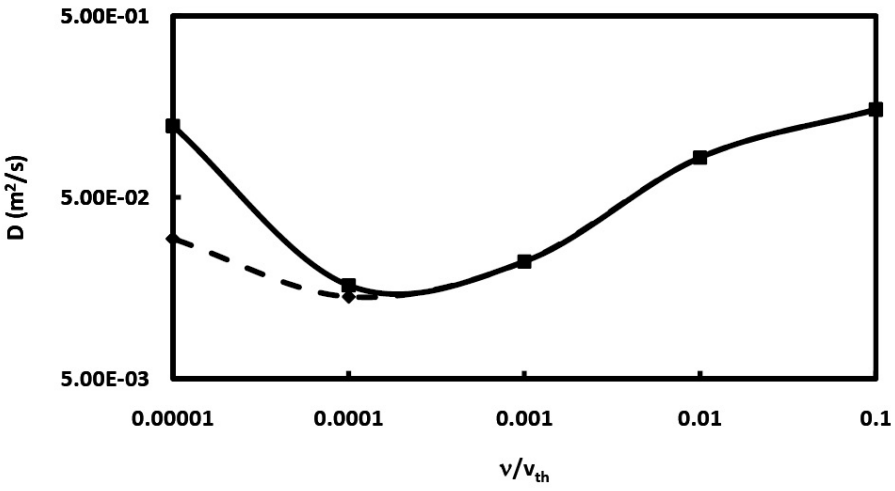

Figure 8. Diffusion coefficients calculated by DKES for the N_p=4, A_p=8 QHS as function of the normalized collision frequencies at ~70% of the radius with a_p~1 m and B~1.2 T. The solid curve is the upper bound of the calculation and the dashed curve is the lower bound.

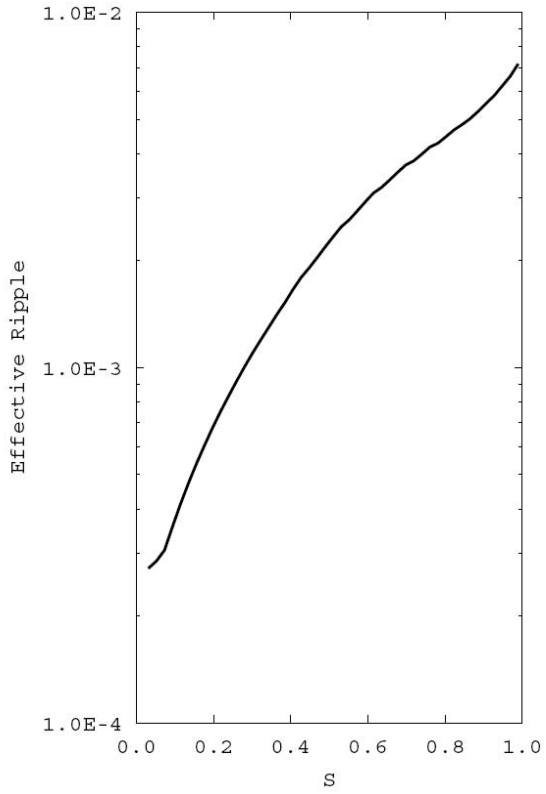

Figure 9. Effect helical ripples as function of the normalized toroidal flux calculated by NEO for the N_p=4, A_p=8 QHS.

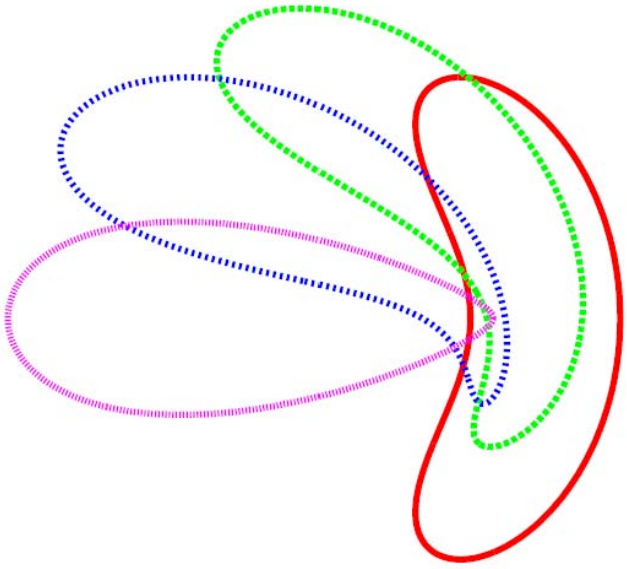

Figure 10. Cross sections of the last closed magnetic surface in four equally spaced toroidal angles for the N_p=5 and A_p=10 QHS.

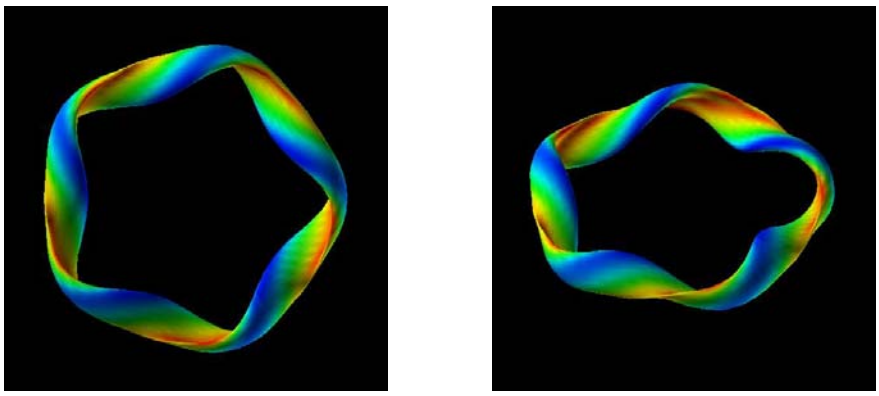

Figure 11. Top and perspective views of the N_p=5, A_p=10 QHS with the magnetic field strength shown in colored contours.

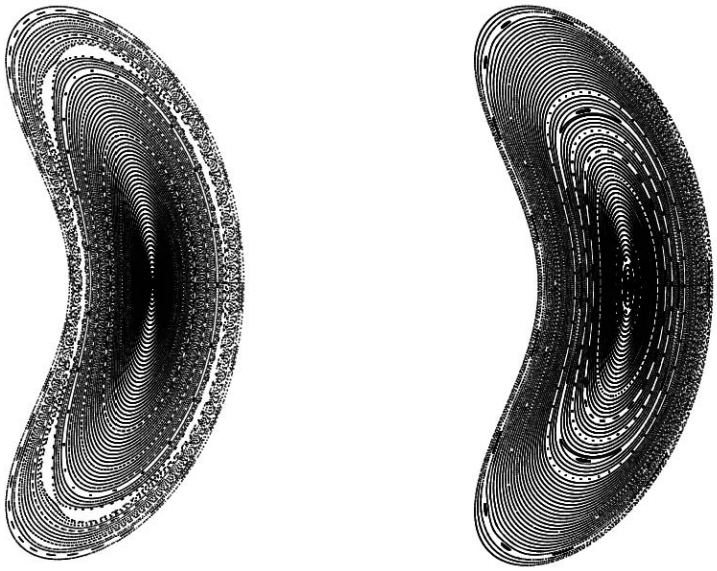

Figure 12. Poincaré plots showing the quality of flux surfaces for the N_p=5, A_p=10 QHS. The left frame is without plasma pressure and currents and the right frame includes the finite pressure effects at 10% β.

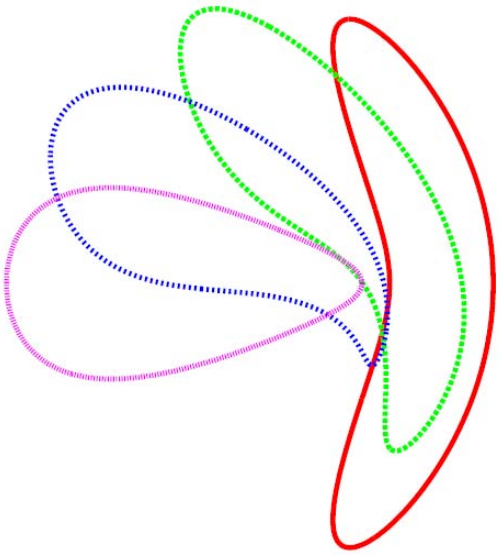

Figure 13. Cross sections of the last closed magnetic surface in four equally spaced toroidal angles for second N_p=5 and A_p=10 QHS discussed in section III.

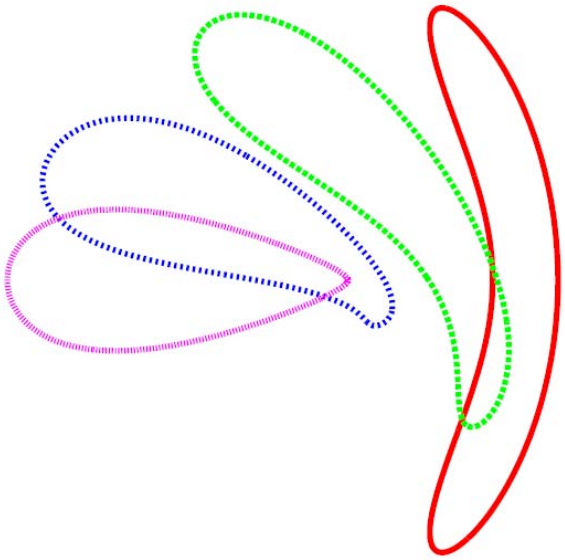

Figure 14. Cross sections of the last closed magnetic surface in four equally spaced toroidal angles for the N_p=3 and A_p=6 QHS having a reduced threshold for MHD stability at 2% β.

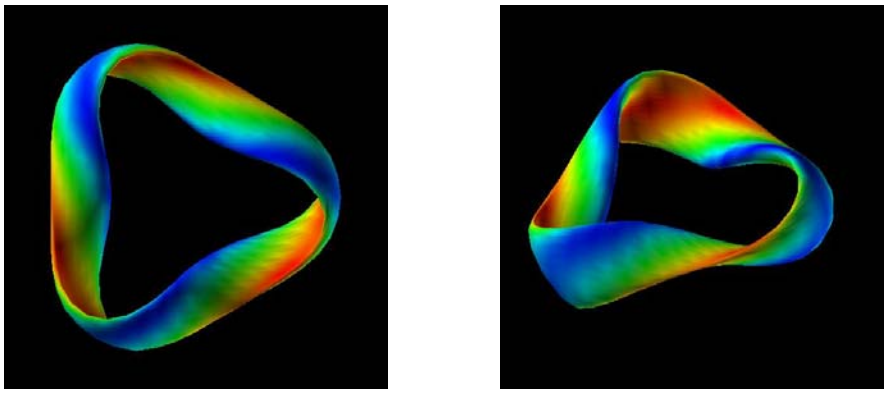

Figure 15. Top and perspective views of the N_p=3, A_p=6 QHS with the magnetic field strength shown in colored contours.

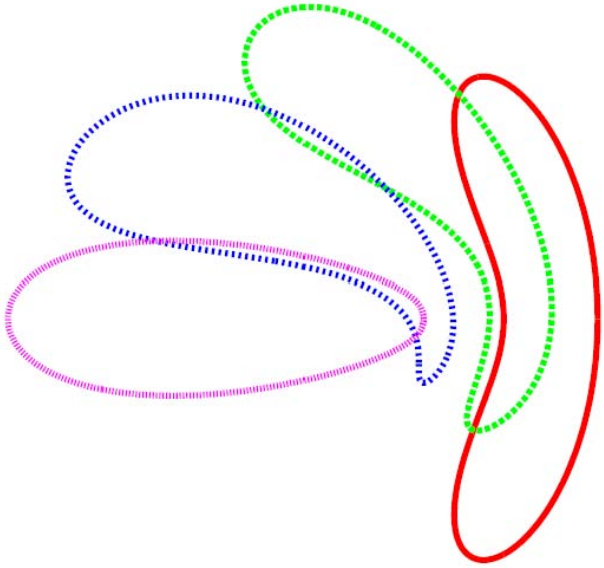

Figure 16. Cross sections of the last closed magnetic surface in four equally spaced toroidal angles for the N_p=3 and A_p=6 QHS which has a threshold for MHD stability at 4% β but with the reduced confinement properties.

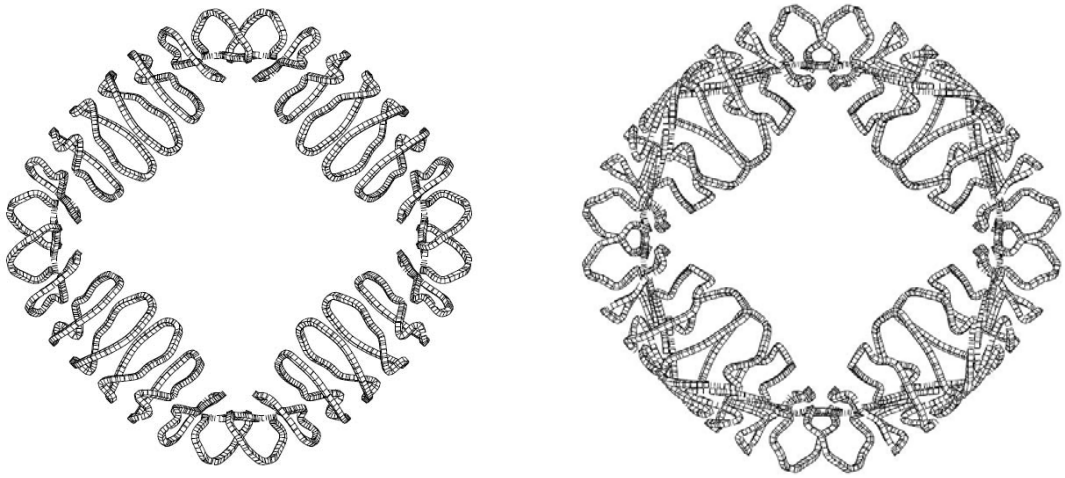

Figure 17. Top views of modular coils for the N_p=4, A_p=8 QHS with four pairs of distinctive coils per field period. The left frame is for a separation distance Δ=0.09R_p between the plasma boundary and the coil winding surface and the right frame is for a separation Δ=0.12R_p, where R_p is the plasma major radius.

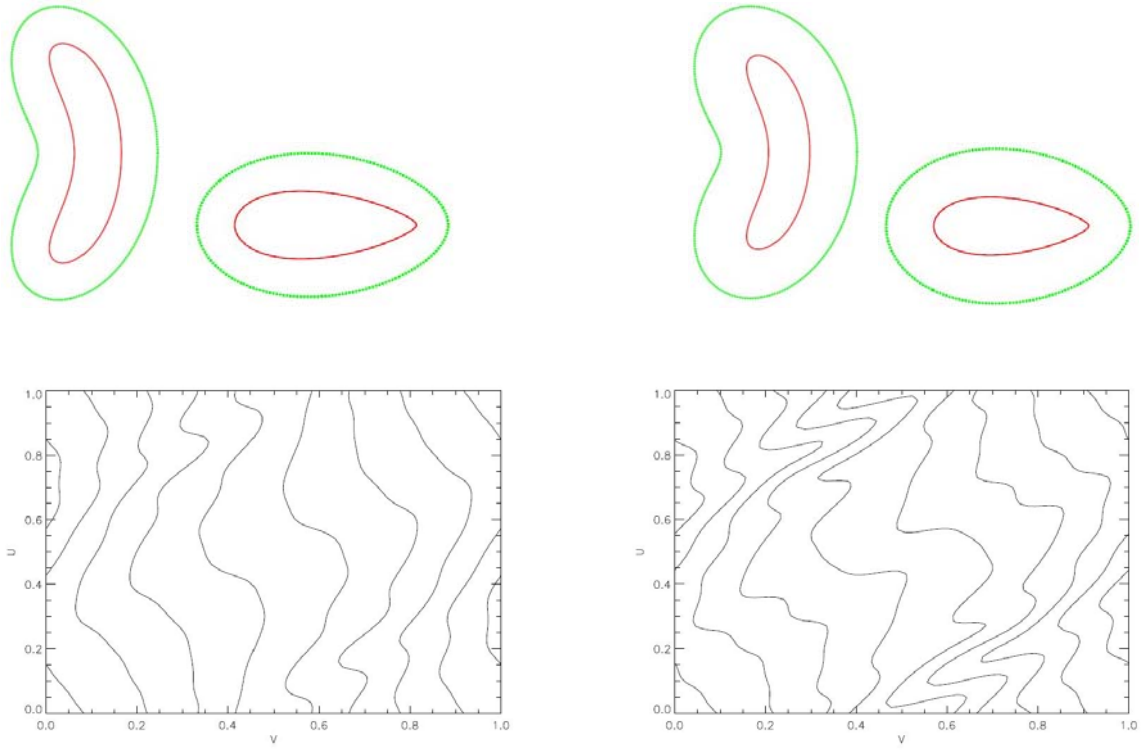

Figure 18. Top row: plasma boundary and coil winding surface at the beginning of a field period and at the half period for separation distances Δ=0.09R_p (left) and Δ=0.12R_p (right). Bottom row: corresponding coil contours viewed on the plane of normalized toroidal (abscissa) and poloidal (ordinate) angles on the winding surfaces.

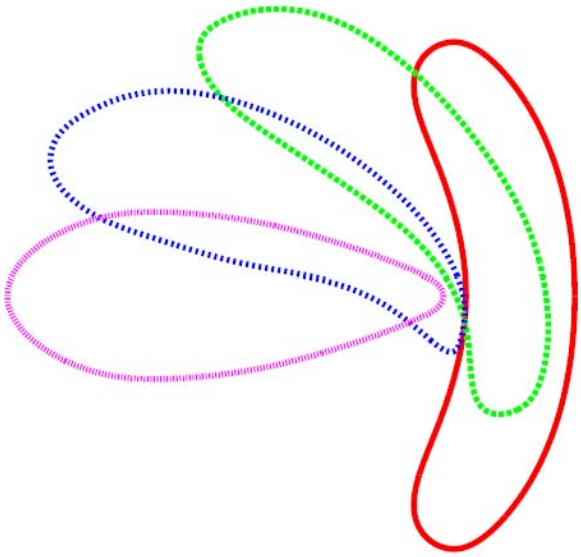

Figure 19. Cross sections of the last closed magnetic surface in four equal toroidal angles over half a period constructed for the N_p=4, A_p=8 QHS using modular coil filaments located at a distance Δ=0.09R_p where R_p is the plasma major radius.

The Princeton Plasma Physics Laboratory is operated
by Princeton University under contract
with the U.S. Department of Energy.

Information Services
Princeton Plasma Physics Laboratory
P.O. Box 451
Princeton, NJ 08543

Phone: 609-243-2245
Fax: 609-243-2751
e-mail: pppl_info@pppl.gov
Internet Address: http://www.pppl.gov